PLOS ONE

RESEARCH ARTICLE

Low cost and open source multi-fluorescence imaging system for teaching and research in biology and bioengineering

Isaac Nuñez[1☯], Tamara Matute[1☯], Roberto Herrera[2], Juan Keymer[3], Timothy Marzullo[2], Timothy Rudge[4]*, Fernán Federici[5,6]*

1 Department of Chemical and Bioprocess Engineering, School of Engineering, Pontificia Universidad Católica de Chile, Santiago, Chile, **2** Backyard Brains, Santiago, Chile, **3** Departamento Ecología, Facultad Ciencias Biológicas; Instituto de Física, Facultad de Física, Pontificia Universidad Católica de Chile, Santiago, Chile, **4** Institute for Biological and Medical Engineering, Schools of Engineering, Medicine and Biological Sciences, Pontificia Universidad Católica de Chile, Santiago, Chile, **5** Departamento de Genética Molecular y Microbiología, Facultad de Ciencias Biológicas, Pontificia Universidad Católica de Chile, Santiago, Chile, **6** Fondo de Desarrollo de Áreas Prioritarias, Center for Genome Regulation, Millennium Nucleus Center for Plant Systems and Synthetic Biology, Pontificia Universidad Católica de Chile, Santiago, Chile

☯ These authors contributed equally to this work.
* trudge@uc.cl (TJR); ffederici@bio.puc.cl (FF)

OPEN ACCESS

Citation: Nuñez I, Matute T, Herrera R, Keymer J, Marzullo T, Rudge T, et al. (2017) Low cost and open source multi-fluorescence imaging system for teaching and research in biology and bioengineering. PLoS ONE 12(11): e0187163. https://doi.org/10.1371/journal.pone.0187163

Editor: Giorgio F Gilestro, Imperial College London, UNITED KINGDOM

Received: August 22, 2017

Accepted: October 14, 2017

Published: November 15, 2017

Data Availability Statement: All sequence and images files are available from the Open Science framework database (https://osf.io/dy6p2/). All the documentation for hardware is available at Docubricks (http://docubricks.com/viewer.jsp?id=701517893260717056). Code is available from GitHUB (www.github.com/synbiouc/fluopi).

Funding: We would like to thank the funders of this study: OpenPlant Fund for financial support to INN, TFM, RHP, JEK, TCM, TJR, and FF; CONICYT Fondecyt Iniciacion 11140776 for providing

Abstract

The advent of easy-to-use open source microcontrollers, off-the-shelf electronics and customizable manufacturing technologies has facilitated the development of inexpensive scientific devices and laboratory equipment. In this study, we describe an imaging system that integrates low-cost and open-source hardware, software and genetic resources. The multi-fluorescence imaging system consists of readily available 470 nm LEDs, a Raspberry Pi camera and a set of filters made with low cost acrylics. This device allows imaging in scales ranging from single colonies to entire plates. We developed a set of genetic components (e.g. promoters, coding sequences, terminators) and vectors following the standard framework of Golden Gate, which allowed the fabrication of genetic constructs in a combinatorial, low cost and robust manner. In order to provide simultaneous imaging of multiple wavelength signals, we screened a series of long stokes shift fluorescent proteins that could be combined with cyan/green fluorescent proteins. We found CyOFP1, mBeRFP and sfGFP to be the most compatible set for 3-channel fluorescent imaging. We developed open source Python code to operate the hardware to run time-lapse experiments with automated control of illumination and camera and a Python module to analyze data and extract meaningful biological information. To demonstrate the potential application of this integral system, we tested its performance on a diverse range of imaging assays often used in disciplines such as microbial ecology, microbiology and synthetic biology. We also assessed its potential use in a high school environment to teach biology, hardware design, optics, and programming. Together, these results demonstrate the successful integration of open source hardware, software, genetic resources and customizable manufacturing to obtain a powerful, low cost and robust system for education, scientific research and bioengineering. All the resources developed here are available under open source licenses.

financial support to FF; CONICYT Fondecyt Iniciación 11161046 for providing support to TJR; Fondo de Desarrollo de Areas Prioritarias (FONDAP) Center for Genome Regulation (15090007) and Millennium Nucleus Center for Plant Systems and Synthetic Biology (NC130030) for providing financial support to FF; CONICYT Fondecyt Regular 1150430 for providing financial support to JEK and Backyard Brains for providing support in the form of salaries for TCM and RHP. The funders had no role in study design, data collection and analysis, decision to publish, or preparation of the manuscript. The specific roles of these authors are articulated in the 'author contributions' section.

Competing interests: Authors TCM and RHP contributed to this work under employment by Backyard Brains, a company that develops and distributes open source scientific equipment. Backyard Brains worked on this project under support of the OpenPlant fund. This does not alter our adherence to PLOS ONE policies on sharing data and materials. Additionally, there are no patents, products in development or marketed products to declare.

Introduction

Fluorescence imaging has become an essential tool for research and education in biological sciences and bioengineering. However, instrumentation for fluorescence imaging is expensive and access to software is often restricted, which imposes a high barrier for democratizing its usage outside academic labs and wealthy research institutions. Open hardware and free/libre and open source software (FLOSS) provides the tools for fabricating these devices at a much lower cost and with better adaptability. The advent of easy-to-use microcontrollers, off-the-shelf electronics and customizable manufacturing technologies such as 3D printers and laser-cutting machines, has given rise to a diverse community of open hardware developers, users and tinkerers. This ethos has facilitated the development of inexpensive scientific devices and laboratory equipment [1–4]; such as PCR thermocyclers [5], photometric sensors [6], a quartz crystal microbalance [7] and neuroscience instrumentation [8–10], among many others [11]. The use of online platforms for project documentation and sharing [12–14], along with the implementation of collaborative practices borrowed from the FLOSS community, is enabling crowdsourced development of advance instrumentation (e.g [15]). These modes of development are lubricated by licenses that guarantee freedom to access, use, modify and distribute source code, design files and derived works.

A broad series of open source digital microscopes and imaging devices have been created (e.g. [16–20]). Some of these include advanced features such as light-sheet illumination [21, 22], two photon scanning [23], a motorized stage [24, 25], optogenetic stimulation [26], cell phone adaptability (e.g. [27–31]), wireless connectivity [32], and cost as little as US$1 [33]. Open source devices for in vivo fluorescence imaging of whole organisms and cell populations are of special interest for spatio-temporal studies [26, 34, 35]. Fluorescence imaging has traditionally relied on broad-spectrum illumination systems, such as mercury lamps, that require channel separation for multicolor imaging. This is usually achieved by switching filters, which involves moving mechanical parts that complicates designs and can cause unwanted vibrations in imaging mainframes. One alternative is to use multiband filters and switch between different wavelength lasers or multiple Light Emitting Diodes (LEDs) whose output can be modulated in microseconds to excite different fluorophores consecutively [36].

Here, we combined low-cost color cameras, off-the-shelf electronics, inexpensive acrylic filters, open-source software, easy-to-use genetic resources, and recently developed long Stokes shift fluorescent proteins to create an integrated imaging system for multiple fluorescence signals from a single excitation wavelength (Fig 1). The device was designed to allow imaging at different scales, ranging from a single bacterial colony (~500–1000 μm) to entire petri dishes (~10 cm), scales not often covered by commercially available devices. We explored the applications and limitations of this system in a series of diverse experimental setups that required spatio-temporal tracking of multiple fluorescence signals. We demonstrate the value and robustness of our system for low cost science, technology, engineering and mathematics (STEM) education, scientific research and bioengineering. All the resources developed here are available under open source licenses.

Materials and methods

DNA construction

All vectors were constructed by Golden Gate using BsaI (NEB) and T4 ligase (NEB). The acceptor vectors for Golden Gate assembly were constructed by Gibson Assembly. Nine level 0 vectors and one acceptor vector compatible with the CIDAR MoClo Toolkit (Addgene) were constructed by Gibson Assembly. The CIDAR MoClo Parts Kit was a gift from Douglas

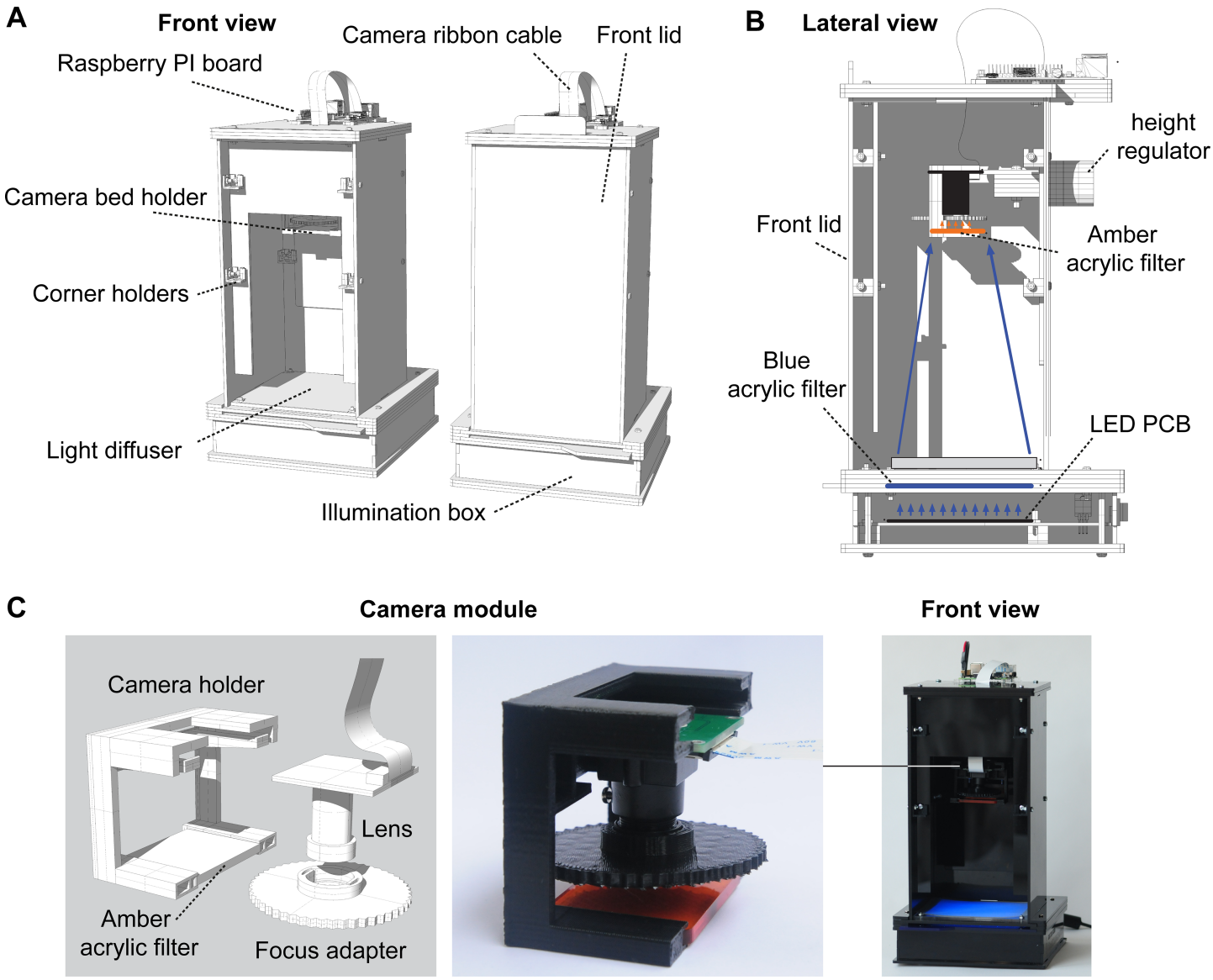

Fig 1. Device general architecture. (A) Schematic rendering of the device with and without the front lid. (B) lateral view of a longitudinal cross-section of the device showing height control, illumination box and filters. (C) Camera and amber filter holder.

https://doi.org/10.1371/journal.pone.0187163.g001

Densmore (Addgene kit # 1000000059). The PCR fragments were amplified using Phusion High-Fidelity ADN Polymerase (NEB) and purified using Wizard SV Gel and PCR Clean-Up System (Promega). The purification of all plasmids was performed using Wizard Plus SV Miniprep DNA Purification System (Promega). All the assembled vectors were checked by colony PCR and later sequenced commercially (Macrogen Inc.). See Table 1 for full description of genetic parts. All genbank files can be dowloaded from the following Open Science Framework link: https://osf.io/dy6p2/.

Growth condition

All tests were carried out on *E.coli* Top10 (Invitrogen) grown at 37˚C in LB medium. Media were supplemented with 1.5% m/v agar for assays on solid media. For inducer applications, we

Table 1. Genetic components used in this study.

Component	Type	Reference
A_J23101_B	Level 0: promoter	This study
J23116_AB	Level 0: promoter	[46]
J23107_AB	Level 0: promoter	[46]
J23100_AB	Level 0: promoter	[46]
R0040_pTet_AB	Level 0: promoter	[46]
A_pLux76_B	Level 0: promoter	This study
A_pLas81_B	Level 0: promoter	This study
R0010_pLac_AB	Level 0: promoter	[46]
BCD2_BC	Level 0: ribosome binding sites (RBS)	[46]
BCD8_BC	Level 0: ribosome binding sites (RBS)	[46]
BCD12_BC	Level 0: ribosome binding sites (RBS)	[46]
B0032m_BC	Level 0: ribosome binding sites (RBS)	[46]
B0033m_BC	Level 0: ribosome binding sites (RBS)	[46]
B0034m_BC	Level 0: ribosome binding sites (RBS)	[46]
B_RiboJ54_C	Level 0: ribosome binding sites (RBS)‘	This study
C_mBeRFP_D	Level 0: coding DNA sequence (CDS)	This study
C_sfGFP_D	Level 0: coding DNA sequence (CDS)	This study
C_CyOFP_D	Level 0: coding DNA sequence (CDS)	This study
C_hmKeima8.5_D	Level 0: coding DNA sequence (CDS)	This study
C_mTurquoise2_D	Level 0: coding DNA sequence (CDS)	This study
C_mRuby2_D	Level 0: coding DNA sequence (CDS)	This study
C_mTFP1_D	Level 0: coding DNA sequence (CDS)	This study
C_luxI_D	Level 0: coding DNA sequence (CDS)	This study
C_lasR C0079_D	Level 0: coding DNA sequence (CDS)	This study
C_lasI_D	Level 0: coding DNA sequence (CDS)	This study
E0030__YFP__CD	Level 0: coding DNA sequence (CDS)	[46]
C0062__luxR__CD	Level 0: coding DNA sequence (CDS)	[46]
B0015_DE	Level 0: Terminator	[46]
D_ECK0818_E	Level 0: Terminator	This study
D_ECK9600_D	Level 0: Terminator	This study
pLac_RiboJ54_YFP_B0015	level 1 vector used in Fig 2A	This study
pLac_RiboJ54_mRuby2_B0015	level 1 vector used in Fig 2A	This study
pLac_RiboJ54_mTurquoise2_B0015	level 1 vector used in Fig 2A	This study
pLac_RiboJ54_mBeRFP_B0015	level 1 vector used in Fig 2A	This study
pLac_RiboJ54_hmKeima8.5_B0015	level 1 vector used in Fig 2A	This study
pLac_RiboJ54_mTFP1_B0015	level 1 vector used in Fig 2A	This study
pLac_RiboJ54_sfGFP_B0015	level 1 vector used in Fig 2A	This study
pLac_RiboJ54_CyOFP_B0015	level 1 vector used in Fig 2A	This study
J23116_BCD12_sfGFP_B0015	level 1 vector used in S1 Fig	This study
J23107_BCD12_sfGFP_B0015	level 1 vector used in S1 Fig	This study
J23100_BCD12_sfGFP_B0015	level 1 vector used in S1 Fig & Fig 2E	This study
J23101_BCD12_sfGFP_B0015	level 1 vector used in S1 Fig & Fig 2E	This study
J23101_RiboJ54_sfGFP_B0015	level 1 vector used in Fig 2E	This study
J23101_RiboJ54_mBeRFP_B0015	level 1 vector used in Fig 2E	This study
J23101_RiboJ54_CyOFP_B0015	level 1 vector used in Figs 2E, 2B, 4 and 6A	This study
J23101_BCD12_mBeRFP_B0015	level 1 vector used in Fig 2E	This study
J23101_BCD12_CyOFP_B0015	level 1 vector used in Fig 2E	This study

(*Continued*)

Table 1. (*Continued*)

Component	Type	Reference
J23101_BCD8_sfGFP_B0015	level 1 vector used in Figs 2E, 2B, 4 and 6A	This study
J23101_BCD8_mBeRFP_B0015	level 1 vector used in Fig 2E	This study
J23101_BCD8_CyOFP_B0015	level 1 vector used in Fig 2E	This study
J23101_BCD2_sfGFP_B0015	level 1 vector used in Fig 2E	This study
J23101_BCD2_mBeRFP_B0015	level 1 vector used in Fig 2E	This study
J23101_BCD2_CyOFP_B0015	level 1 vector used in Fig 2E	This study
J23101_B0034_sfGFP_B0015	level 1 vector used in Fig 2E	This study
J23101_B0034_mBeRFP_B0015	level 1 vector used in Figs 2E, 2B, 4 and 6A	This study
J23101_B0034_CyOFP_B0015	level 1 vector used in Fig 2E	This study
J23101_B0033_sfGFP_B0015	level 1 vector used in Fig 2E	This study
J23101_B0033_mBeRFP_B0015	level 1 vector used in Fig 2E	This study
J23101_B0033_CyOFP_B0015	level 1 vector used in Fig 2E	This study
J23101_B0032_sfGFP_B0015	level 1 vector used in Fig 2E	This study
J23101_B0032_mBeRFP_B0015	level 1 vector used in Fig 2E	This study
J23101_B0032_CyOFP_B0015	level 1 vector used in Fig 2E	This study
12X	level 1 acceptor vector	This study
1LU2	vector used in Fig 3	This study
plac34lasI	vector used in Fig 3	This study
plac34luxI	vector used in Fig 3	This study
plac54lasI	vector used in Fig 3	This study
plac54luxI	vector used in Fig 3	This study
plas8O	vector used in Fig 3	This study
plas33O	vector used in Fig 3	This study
plux34G	vector used in Fig 3	This study
plux54G	vector used in Fig 3	This study
ptet32LasR	vector used in Fig 3	This study
Std34BeRFP	vector used in Fig 3	This study

https://doi.org/10.1371/journal.pone.0187163.t001

prepared a stock solution of 0.1 M IPTG, sterilized by 0.22 mm filter. Antibiotics were used as solutions of kanamycin (50 ug/ml) and carbenicillin (100 μg/ml).

Different fluorescent proteins were tested by streaking transformed cells onto petri dishes from glycerol stocks and growing them for 24 hrs at 37˚C. Expression was induced with 30 μl of 0.1M IPTG.

Transformation and co-transformation

The chemocompetent cells used for all the transformations were made by the CCMB80 method in *E.coli* Top10 (Invitrogen) (OpenWetWare: "TOP10 Chemically competent cells", 2013). Cells stored at -80˚C were thawed on ice for 20 minutes. For single transformations, a 1 μl of plasmid stock (concentration ~ 1ng/μl) was added to 50 μl of chemocompetent Top10 *E. coli*. In the case of co-transformations, 100 ng total of each plasmid were mixed with deionized water to obtain a final volume of 6 μl, which were then added to 50 μl of chemocompetent Top10 *E. coli*. The cells were incubated for 25 minutes and heat-shocked at 42˚C for 1 minute, after which they were incubated on ice for an additional 2 minutes.

A 250 μl volume of LB medium was added to each transformation and incubated with shaking (250 rpm) at 37˚C. The incubation time for the single transformation was 1 hour, after

which a volume of 25 μl of transformed cells was plated in solid LB medium supplemented with antibiotics. In the case of co-transformations, the incubation time was 1.5 hours, after which 35 μl of transformed cells were plated on LB-agar supplemented with antibiotics. Plates were incubated at 37˚C overnight (~ 12–16 hours) for colony formation.

Colony-sectoring assay

Cultures of the three TOP10 cells containing the different vectors were grown overnight and mixed proportionally. The culture mixture was diluted 1:100 or 1:10,000 and a 0.5 μl drop was placed in the center of a petri dish. Plates were then incubated at 37˚C for 12 hours and imaged every 12 hours for 7 days at room temperature.

We have created a protocol online describing this experimental procedure in more details (dx.doi.org/10.17504/protocols.io.jsecnbe).

Grown-on-membrane assays

An ISO-GRID membrane filter (Neogen corporation, 1600 Grid 0.45μm, 36 Grid; product #6802) was placed on top of LB agar plates, with the hydrophobic grid facing up. Bacteria co-transformed with the sender/receiver plasmids were grown at 37˚C in LB liquid media to OD600 0.03 (~5 hours) and 0.5 μl of cell culture was pipetted within each well following arrangements that depend on the assays. We have created a protocol online describing this experimental procedure in more details (dx.doi.org/10.17504/protocols.io.jsfcnbn).

Mix colonies time lapses

Time lapses and experiments shown in Figs 4 and 5 were performed by mixing liquid cultures of the different strains transformed with mBeRFP, CyOFP1 and sfGFP (eg, 100 μl of each one), performing three consecutive 1:100 volume dilutions of the culture (pure or mixture) and plating this mixed culture on a LB agar plate. We have created a protocol online describing this experimental procedure in more details (dx.doi.org/10.17504/protocols.io.jsucnew).

Camera settings

For Fig 2 and Fig 3 the camera was operated using the command raspistill as follows:

Fig 2A: raspistill -t 4000 -ss 90000 -ISO 300 -awbg 1,1 -co 50 -o

Fig 2B raspistill -t 5000 -ss 3000 -o

Fig 3A to 3D: raspistill -t 4000 -ss 100000 -ISO 300 -awbg 1,1 -co 60 -o

Fig 3E: raspistill -t 4000 -ss 70000 -ISO 300 -awbg 1,1 -co 40 -o

and raspistill -t 4000 -ss 50000 -ISO 300 -awbg 1,1 -co 30 -o

Time lapses and experiments shown in Figs 4 and 5 were performed with python code controlling the camera as described in text.

Results

Hardware design

To allow for full customization, the mainframe was developed as enclosures made of editable laser-cut 3mm acrylic pieces (S1 File). These can be easily stacked and shipped since they are mostly flat. The imaging device was assembled by holding together the acrylic plates with small 3D printed corner holders, designed to be used with standard nuts and bolts that can be

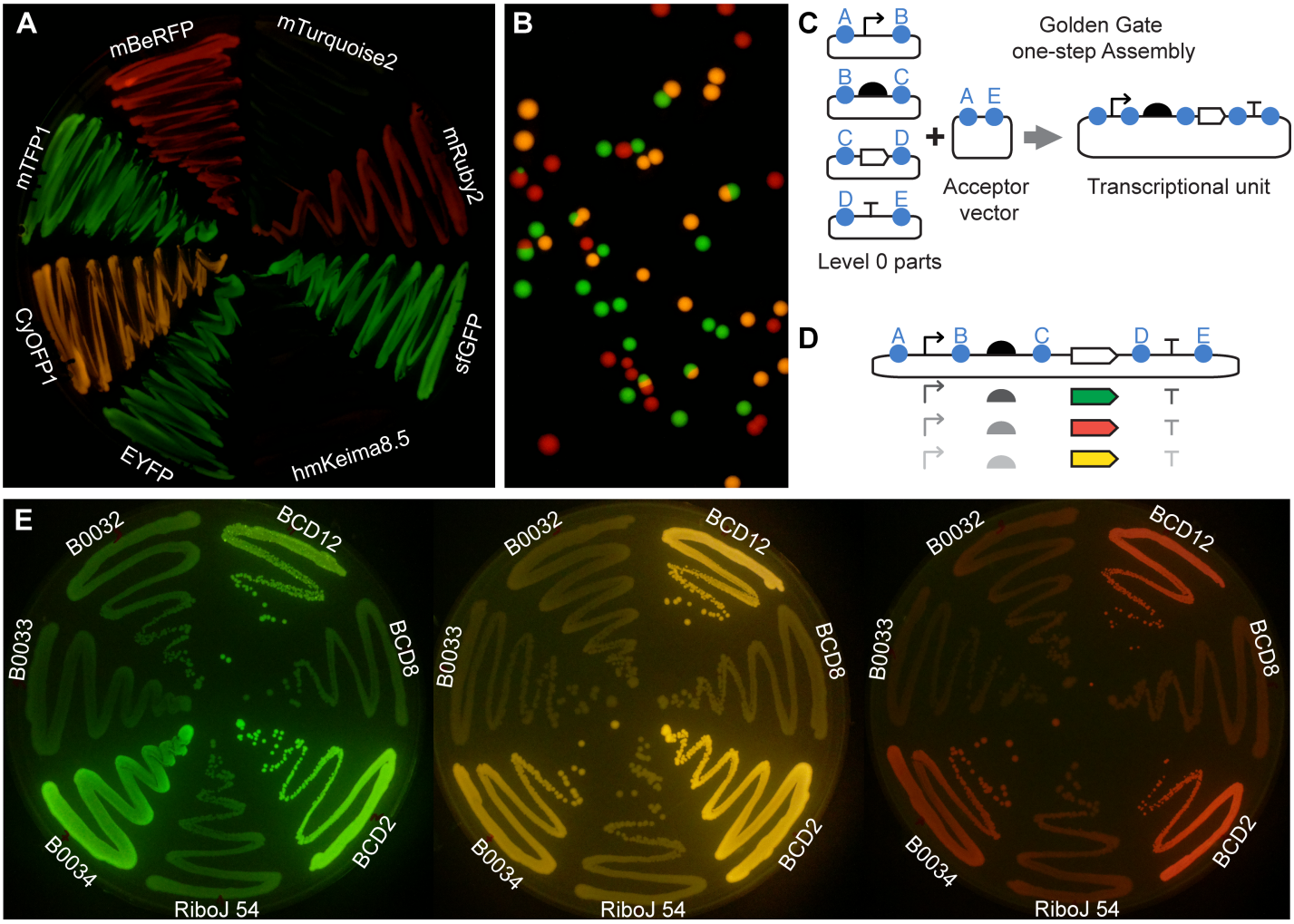

Fig 2. Simultaneous imaging of different fluorescent proteins with single excitation at 470 nm. (A) CyOFP1, hmKeima8.5, mBeRFP, mRuby2, mTFP1, sfGFP, mTurquoise2, and EYFP, with R0010 promoter and RiboJ 54 insulator-RBS treated with (right) and without (left) IPTG. (B) Representative image showing growing E. coli colonies expressing sfGFP, CyOFP1 and mBeRFP. (C) Schematic representation of Golden Gate one-step assembly for the construction of genetic systems from level 0 parts. (D) Schematic representation of combinations of promoter, ribosome binding sites (RBS), coding DNA sequence (CDS) and terminator that can be assembled with the standardized Golden Gate method. (E) Image of agar plates with streaks of *E. coli* expressing sfGFP, CyOFP1 and mBeRFP under J23101 promoter and different ribosome binding sites (RBS): BCD12; BCD8; BCD2; RiboJ54; B0034; B0033; and B0032. B0015 terminator was used for all the constructs. No post-editing has been applied to these images; only cropping and alignment.

https://doi.org/10.1371/journal.pone.0187163.g002

replaced depending on local supply. All 3D printed parts were designed considering the FDM process: using mostly horizontal and vertical faces, low inclination angles and no "ceilings", therefore no support structures were needed. The object architecture is fully modular (S1 File).

The top module supports the Raspberry Pi 3 computer for camera control (Fig 1A) (S2 File). The top enclosure also provides support to the camera bed, height regulator and camera holder (S3 File). The camera holder also supports an acrylic emission filter in front of the lens and a focus adapter wheel for manual adjustable focus lens (Fig 1B and 1C). Recorded images are transmitted to the Raspberry Pi with a standard 15 pin (300 mm) ribbon cable. Height adjustment works with a standard bolt and nut mounted with a knob, which slides up and down tightens for fixation on the back plate of the module. The maximum height of the

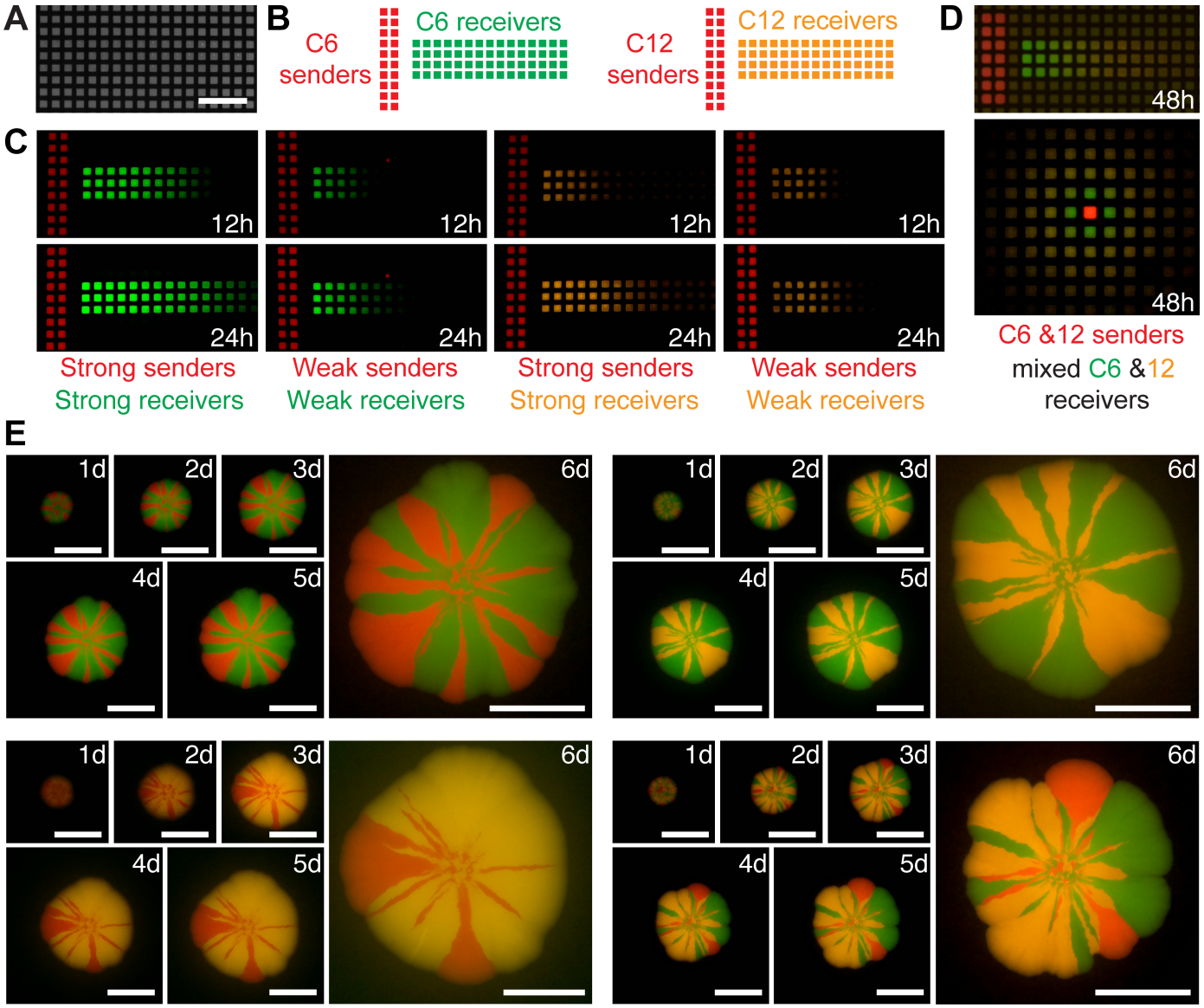

Fig 3. System testing under different experimental setups. (A) Image of ISO-GRID permeable membrane used in experiments shown in B to D. Scale bar, 1000 μm. (B) Schematic representation of diffusion assay for *E. coli* cells producing ("sender cells") and responding to ("receiver cells") C6 and C12 homoserine lactones plated on permeable membranes printed with hydrophobics grid lines. (C) Images of a time-lapse experiment of cell responses to C6 and C12 homoserine lactones. Images were taken at 12 and 28 hours after plating. Cells were grown at 37˚C outside the device. Vector co-transformation for: strong C12 receiver, pTet_32 LasR + pLas8O; weak C12 receiver, pTet_32 LasR + pLas33O; strong C6 receiver, 1LU2 + pLux34G; weak C6 receiver, 1LU2 + pLux54G; strong C6 sender, Std34BeRFP + pLac34LuxI; weak C6 sender, Std34BeRFP + pLac54LuxI; strong C12 sender, Std34BeRFP + pLac34LasI; weak C12 sender, Std34BeRFP + pLac54LasI. See Table 1 for sequence information. Scale bar, 1000 μm. (D) Images at 48h after plating a mix of C6 and C12 sender cells (expressing mBeRFP, in red) and a mix of C6 and C12 receiver cells expressing sfGFP and CyOFP, respectively. ROH: pTet_32 LasR + pLas8O. (E) Colony-sectoring assay. Strains labelled with CyOFP1, mBeRFP and sfGFP fluorescent proteins seeded on agar LB plates in combinations of two (CyOFP1-mBeRFP, CyOFP1sfGFP and sfGFP-mBeRFP) or three (CyOFP1, mBeRFP and sfGFP) and tracked every 24h for 6 days. No post-editing has been applied to these images; only cropping and alignment. Scale bar, 500 μm.

https://doi.org/10.1371/journal.pone.0187163.g003

imaging system allows the camera module to get images as wide as the illuminated area at the base of the top module, designed to fit a 90mm standard petri dish. The adapter wheel at the lens permits correcting for focus when height is changed. Together, the top enclosure maximizes the use of space while providing light-blockage for complete darkness during imaging

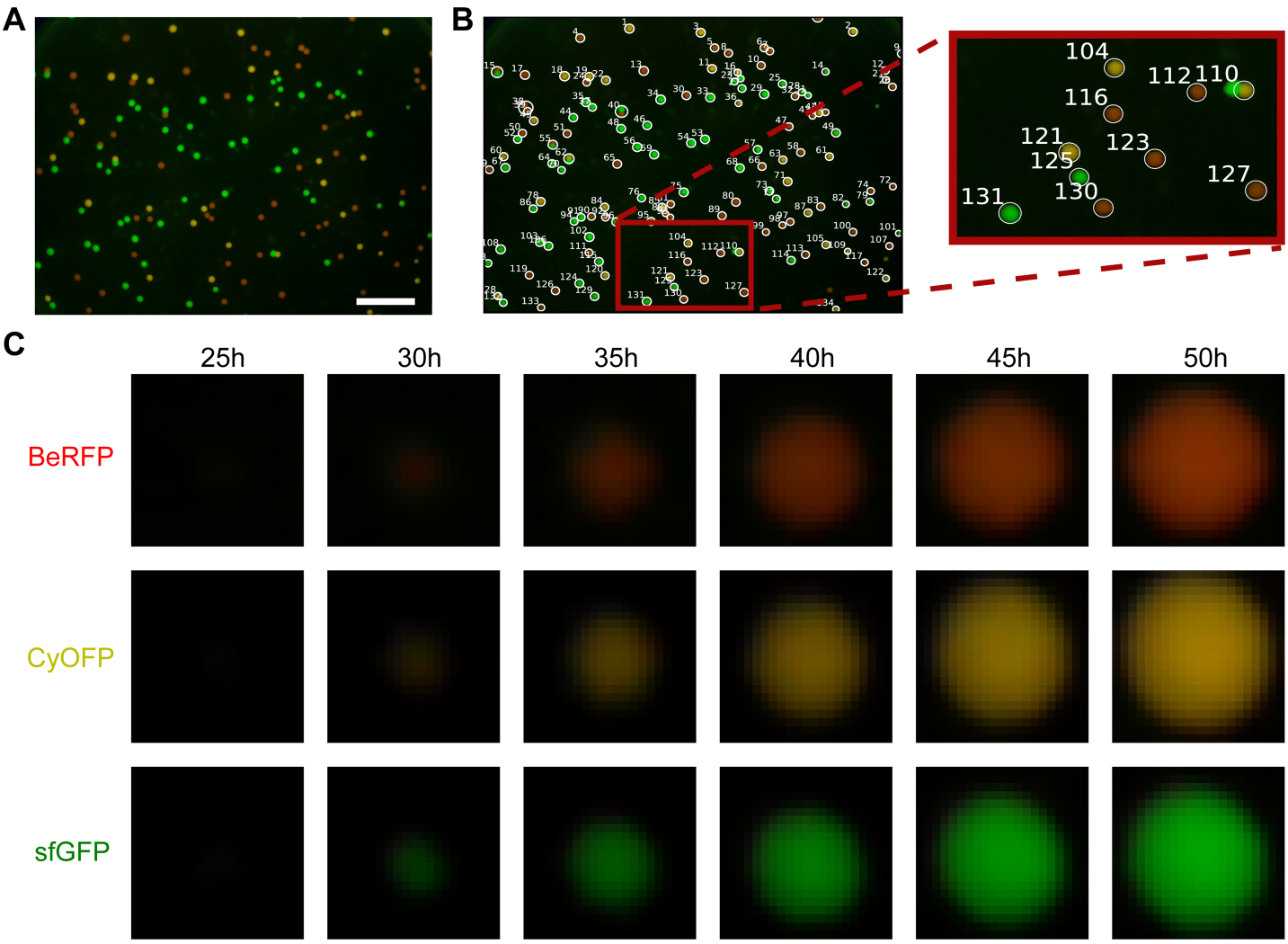

Fig 4. Colony identification and segmentation from timelapse images. A) Endpoint timelapse image (see S4 Movie) of a plate with growing colonies of three different strains, each one expressing a different fluorescent protein. Scale bar = 1cm. B) Colony identification (label them with an ID), by getting position in the image and final size. C) Segmentation of regions of interest (ROIs) defined by the standard deviation of the identified blobs. One example of each strain is shown.

https://doi.org/10.1371/journal.pone.0187163.g004

(Fig 1C). The 3D printed adaptor that encloses the camera module is detachable, allowing for standalone use, transforming the camera in a powerful microscope and visualizer by its own, not described in this project.

The bottom module, inspired by open source blue transilluminators used for DNA electrophoresis gels [37], holds the illumination system composed of a matrix of 100 blue (470 nm) 5 mm LEDs. We designed a printed circuit board ("PCB") to operate these LEDs, which also supports components for analog and digital on/off control (S4 File). For digital control, a TIP122 transistor was used, considering 3.3 volts for the Raspberry GPIO control. A regulable 12–24 volts power supply was chosen so the PCB required less components (using 5 LEDs in parallel for a resistor) and there would not be a need for additional security requirements (i.e. a fuse). The excitation filter is housed in between the top plates of this enclosure and is fastened between the top adjusting screws and the main mounting screws on the base (Fig 1B). This is a

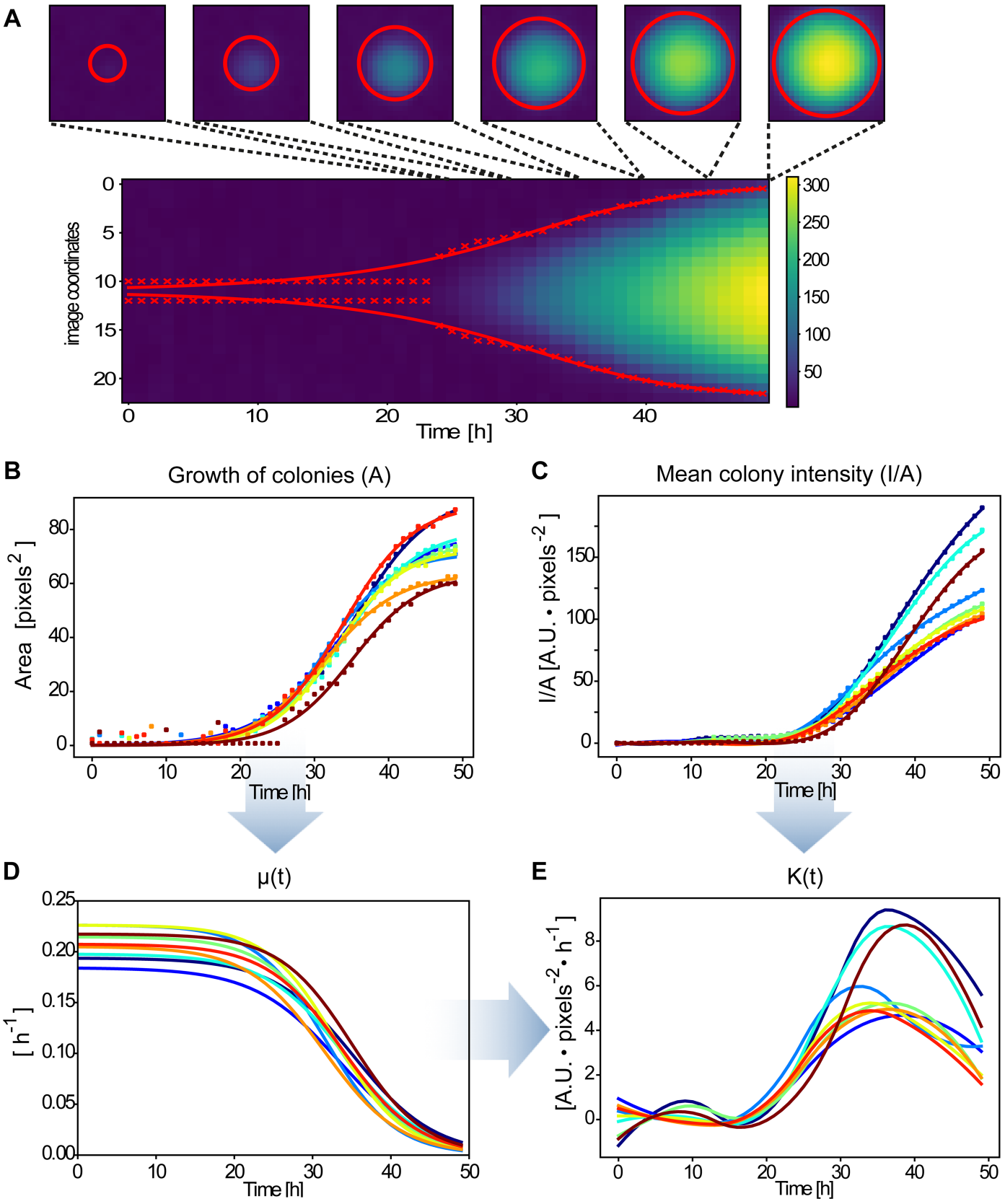
A
image coordinates
Time [h]
B
Growth of colonies (A)
Area [pixels^2]
Time [h]
C
Mean colony intensity (I/A)
I/A [A.U. • pixels^{-2}]
Time [h]
D
μ(t)
[h^{-1}]
Time [h]
E
K(t)
[A.U. • pixels^{-2} • h^{-1}]
Time [h]

Fig 5. Analysis and parameter estimation from identified colonies. (A) kymograph of the pixel signal in the central slice of an example colony. The x marks show the radius estimated for each time and the red line is the radius value obtained from a fitted area function (also red circles). (B) Colony area curve fitting for some example colonies. Dots are the estimated area from the standard deviation of the blobs and the continuous lines are the model fitting of this values (C) Mean fluorescence intensity signal over time for the example colonies. Lines were obtained by spline smoothing. (D) Colony growth rate estimation from the data for each selected colony. (E) Protein expression rate parameter estimation using the previous data.

https://doi.org/10.1371/journal.pone.0187163.g005

blue 3 mm acrylic that slides in from the front, allowing the filter to be exchangeable. The distance between this blue filter and the LEDs was optimized to obtain an even distribution of light on the diffuser that sits at top of the bottom module. Care should be taken to ensure an even distribution of light if redesign of the bottom module is needed (e.g. varying the height between LEDs and diffuser/blue acrylic). The top module mounts on the bottom module by sliding in from the front and secures with the top adjusting screws. Please see http://docubricks.com/viewer.jsp?id=701517893260717056 for detailed assembly instructions and full description of the pieces.

Genetic resources for simultaneous imaging of multiple fluorescent signals under single excitation/emission setup

In order to obtain multiple fluorescent signals simultaneously from a single excitation wavelength and a fixed filter, we evaluated a series of fluorescent proteins potentially excitable at 470 nm and detectable with the amber filter (Fig 2A). We tested CyOFP1 [38], hmKeima8.5 [39], mBeRFP [40], mRuby2 [41], mTFP1 [42], sfGFP [43], mTurquoise2 [44], EYFP [45]. We took images at different camera settings and evaluated their performance. For full transparency, none of the images shown in this work was edited. We selected sfGFP (ex 485/em 510) and the long stokes shift fluorescent proteins CyOFP1 (ex 497/em 589) and mBeRFP (ex 446/em 611) since they showed distinguishable signals in colonies of *Escherichia coli* grown in the same plate (Fig 2B). mTurquoise2 and hmKeima8.5 did not show detectable signals (Fig 2A).

All these fluorescent proteins, as well as all regulatory sequences (e.g. promoters, RBSes, terminators), developed in this work were created as modular parts standardized for fast, combinatorial and efficient fabrication of genetic constructs. In particular, we domesticated these components as "level 0" components following the CIDAR MoClo standards for Golden Gate assembly DNA assembly [45] (Fig 2C). This design also made our resources compatible with hundreds of parts distributed in other registries and labs (e.g. [46]). This method allowed us to combine the chosen fluorescent proteins with different regulatory elements (Fig 2D). We were able to test different ribosome binding sites (Fig 2D) and promoters (S1 Fig).

In order to demonstrate the range of possible applications of our system, we tested different experimental setups using the Raspberry Pi camera software (RPI foundation). First, we imaged DNA electrophoresis gels loaded with different volumes of 1 kb DNA ladder; obtaining signal detection in the range of volumes often used in DNA gel electrophoresis (e.g. 4–6 μl) (S2 Fig). Next, we tested the detection of spatio-temporal fluorescent signals as a consequence of artificial cell–cell communication based on 3-oxo-C6- and 3-oxo-C12 homoserine lactones (HSLs). Bacterial cells that produce (i.e. senders) and respond to (i.e. receivers) homoserine lactones were plated within wells outlined by hydrophobic ink on permeable membranes (ISO-GRID membrane filters) (Fig 3A–3D). These grid membranes were placed on top of agar plates containing growth media (Fig 3A). This setup allows for cell containment in each well while permits the diffusion of the homoserine lactones through agar to neighboring wells (Fig 3B). Then, cellular responses to diffusive signals were tracked over time [47].

In order to provide resources that permit full flexibility in the construction of cells that produce and/or respond to these signals, we created level 0 parts for: i) LuxI and LasI enzymes, in charge of the synthesis of C6 and C12 homoserine lactones, respectively. ii) LuxR and LasR genes, in charge of binding and responding to C6 and C12 HSLs, respectively. and iii) pLux and pLas promoters, from which transcription is induced by LuxR/LasR in response to C6-HSL or C12-HSL respectively. With these tools, we created strong and weak senders and receivers of both signals and registered their behaviour in time (Fig 3C). The imaging system showed good contrast and permitted to track CyOFP1, mBeRFP and sfGFP fluorescent signals simultaneously. Moreover, this system allowed us to track and distinguish the responses of mixed populations of C6 and C12 senders/receivers (Fig 3D).

Next, we evaluated an experimental design used in microbial ecology studies, colony-sectoring assay, in which a mix of bacterial strains is inoculated as a single drop on a petri dish and the dynamics of their growth registered in time lapse [48, 49] (Fig 3E). Strains labelled with CyOFP1, mBeRFP and sfGFP fluorescent proteins were plated in pairs and triplets. These plates were grown in a 37˚C incubator and imaged every 24h over 6 days. Since the device is modular and customizable, we were able to use a shorter top module for the last image at 6 days that permitted a closer position to the plate (see hardware description). The system permitted good detection and discrimination of the three signals. All images were taken with the same settings (described in materials and methods). Under these standard conditions, the CyOFP1-mBeRFP combination showed some background noise in the last image. None of these images has been edited, with the aim of showing raw data produced by our system. These data demonstrate the utility of our system for experimental setups commonly used microbiology, synthetic biology and microbial ecology studies.

Open-source software for hardware control and data analysis

We developed simple python code to operate hardware, run time-lapse experiments and store resulting image sequences (e.g. S1–S3 Movies), which is available via Github (https://github.com/SynBioUC/FluoPi; see folder "Hardware_control"). We also created an extensive Python module (fluopi) with functions for analyzing and visualizing these image sequences. We made extensive use of existing open-source projects Numpy, Scipy, Matplotlib, and Scikit-image, as well as the Raspberry Pi foundations python modules.

Separately, we provide example Jupyter (IPython) notebooks containing code for analysis of time-lapse image series that contain detailed explanation of the analysis process. A simple tutorial notebook introduces the concepts used in loading images and processing them to extract biologically meaningful information (see "Image_processing.ipynb" in folder "Tutorials"). We also provide a simple tutorial notebook describing how to control the imaging hardware from Python (see "FluoPi_control_timelapse.ipynb" in folder "Tutorials"). *Jupyter* provides an intuitive and interactive way to run and develop Python code while immediately viewing the results. As such, these notebooks are ideal for teaching classes or as an introductory tutorial for those students new to programming.

Below we show how this open source software is used to find the location of colonies, estimate their size, growth-rate, and fluorescence and from these data extract the rate of gene expression.

Images data management and colony slicing

Timelapse image sequences of bacterial colonies expressing fluorescent proteins contain valuable data about growth, gene expression and possible inter-colony interactions. The first step

in extracting this information is to process images to generate separate signals for each colony's size and fluorescence.

The images are composed of three channels—red (R), green (G), blue (B) -, each of which can contain different information about the cells and is managed separately. We created a Jupyter notebook to analyze timelapse images of growing colonies constitutively expressing different fluorescent proteins (Fig 4A, S4 Movie) as an example of the kind of data it is possible to obtain with FluoPi and the fluopi Python module. We provide a simplified tutorial demonstrating the principles and mathematical analysis behind the Python module (see "Colony_size_and_fluo.ipynb" in folder "Examples").

The first steps in the analysis involve data management, essential for teaching programming: reading the image files and organizing their data in arrays. Next image processing is introduced to remove the background signal, sum all the channel values over time for each pixel, and smooth the data with a gaussian filter. After this pre-processing a gaussian shape ("blob") detector from *skimage* is used to find the position of each colony in the plate and assign labels to them (Fig 4B). With the standard deviation of these blobs it is possible to define square regions of interest (SROIs) where colonies are situated (Fig 4C) and allows management of each of them separately.

Growth and fluorescent expression rate of colonies

From the data extracted from images as described above, it is possible to estimate the growth rate of each colony and the average constitutive gene expression rate of a fluorescent reporter, considering multiple colonies on a single plate. To get growth information—size (area) and growth rate (relative change in area) -, it is possible to approximate the colony size by the region expressing fluorescent signal. This size can be obtained by applying the gaussian blob detector to each SROI in all frames (i.e. time points), obtaining the colony radius/area over time (Fig 5A). The result is noisy, mainly at the beginning, and so we fit the sigmoidal area model in Eq (1) to the area values computed with the above radii (Fig 5B).

$$A(t) = \frac{A_{max}}{1 + e^{-\mu_{max}(t-t_0)}} \tag{1}$$

Then, as growth rate is defined by Eq (2), we are able to directly estimate the growth rate of the colonies with Eq (3) as shown in Fig 5D

$$\mu(t) = \frac{1}{A(t)}\frac{dA(t)}{dt} \tag{2}$$

$$\mu(t) = \frac{\mu_{max}}{e^{\mu_{max}(t-t_0)} + 1} \tag{3}$$

On the other hand, we show (see S5 File) that the fluorescent expression rate, proportional to protein expression rate, is given by:

$$K_F(t) = \frac{d(I/A)}{dt} + \mu \cdot (I/A) \tag{4}$$

Then, we need to compute the mean intensity signal per unit of area (I/A). To achieve this, we get the colony fluorescent intensity in each frame by summing the three channel values for each pixel inside its computed area. Then dividing by the total number of pixels within this area it is possible to get the mean fluorescent intensity in each time step (Fig 5C). These values were smoothed by applying a smoothing spline function (scipy.interpolate.UnivariateSpline),

which allows to compute analytically its derivatives with respect to time. Finally, with all these values, we are able to characterize the fluorescent protein dynamics by estimating the fluorescent reporter expression rate (Fig 5E).

Distinguishing multiple fluorescent proteins from R,G,B color channels

An interesting aspect of being able to detect diverse fluorescent proteins is the possibility to label and identify different strains expressing them. To do this we first extract colony fluorescence signals as described above. With this data it is possible to get the characteristics of each fluorescent protein and classify the colonies according to strain.

These signals are in three channels, nominally labelled "red", "green" and "blue" and depend on the filters and sensitivity of the camera. Each fluorescent protein has a characteristic spectrum which overlaps with these three channel spectral sensitivities. If we assume a linear relation between fluorescent protein expression and intensity of signal, it is possible to find a characteristic linear relation between the intensities in the (R,G,B) channels of each fluorescent protein (see S6 File). That is, the relative intensity of each fluorescent protein in the (R,G,B) channels is distinct.

To test this, we performed independent timelapse experiments of strains expressing sfGFP, CyOFP and BeRFP (Fig 6A, S5–S7 Movies), from which we computed a characteristic linear relation for the emission of each protein in the red and green camera channels (Fig 6B). To test the capability of classification of this approach, we performed another timelapse with a mix of the three strains and classified each colony accord the closest characteristic linear relation between red and green camera channels (Fig 6C) (S8 Movie). This classification could be a useful tool to compute and compare attributes between groups of strains especially for microbial ecology studies. We provide a simplified jupyter notebook describing these procedures in an interactive way (see "Colony_classification_full.ipynb" in folder "Examples").

Discussion

Following the impact of FOSS in software development, open hardware aims to democratize and accelerate hardware development in a similar manner. The scientific community has started to embrace this approach; with hundreds of labs around the globe designing and making their own equipment (e.g. [50]). Often these designs replace commercial scientific instrumentation, and self-manufacturing can reduce costs by 90–99% [4, 51], resulting in hundreds to thousands percent return on investment in science funding [52]. The total cost of our device is approximately US$250, including all components, materials, 3D printing and CNC cutting service fees. Commercial equivalents can cost as much as US$10000 with less functionality. Reducing costs and using accessible components lowers the access barrier to scientific experiments and democratizes science. In this way, open hardware engages talented developers and experimenters from non-traditional environments such as those in high schools, DIY movements, maker spaces, biohacking communities and art collectives (e.g. [14] [53–57]).

The open source nature of our project aims to contribute to and benefit from these non-traditional scientific communities, especially from the DIY microscopy community (e.g. [58]). To facilitate this process, we have provided full documentation of assembly steps (http://docubricks.com/viewer.jsp?id=701517893260717056) and operational code (github.com/synbiouc/fluopi). Good documentation is critical for crowdsourced design improvements. It also permits adaptations to local needs and restrictions, for example due to availability of parts, and facilitates the incorporation of new parts adapted from other open source projects. For instance the use of an adjustable focus RPI camera, instead of a fixed lens mounted on the

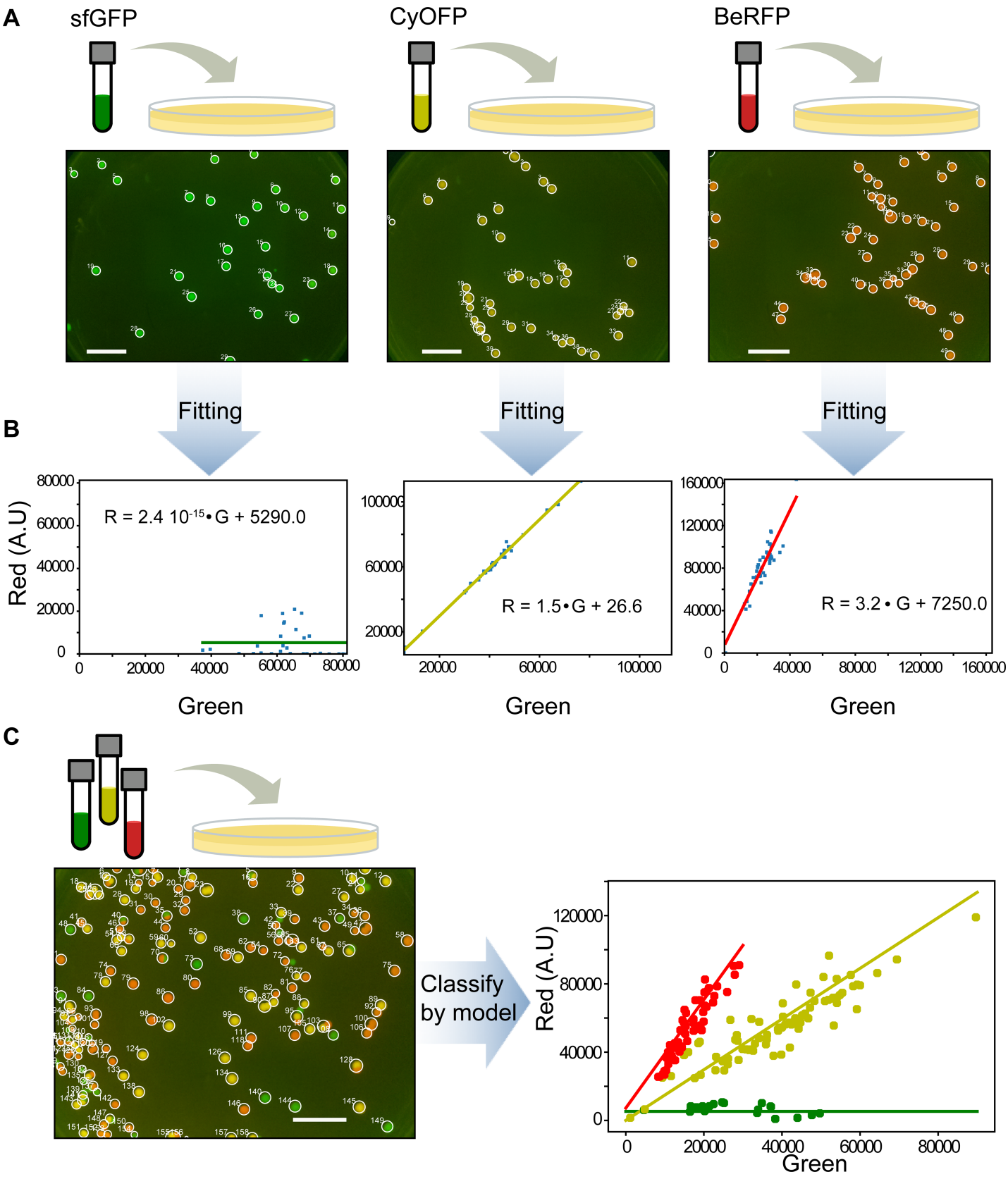
A
sfGFP
CyOFP
BeRFP
Fitting
Fitting
Fitting
B
Red (A.U)
R = 2.4 10-15 • G + 5290.0
R = 1.5 • G + 26.6
R = 3.2 • G + 7250.0
Green
Green
Green
C
Classify by model
Red (A.U)
Green

Fig 6. Distinguishing different strains by (R,G) color profile. (A) Timelapse images were taken separately of three strains, each expressing a different fluorescent protein (sfGFP, BeRFP and CyOFP). Figure shows final image (see S5–S7 Movies) with the detected colonies labeled. Scale bar = 1cm. (B) Characteristic linear relationship between red and green channel for each strain/fluorescent protein obtained from each timelapse in A. Each dot is the (R,G) total signal pair of a colony and the straight line is the linear regression. (C) When grown together on the same plate, the characteristic profile obtained could be used to classify the colonies according to strain/fluorescent protein (see S8 Movie). Scale bar = 1 cm.

https://doi.org/10.1371/journal.pone.0187163.g006

Raspberry PI V2 camera, was suggested to us by another group working on similar developments (FlyPi microscope; [26]).

The imaging device is fully modular (S1 File), permitting the re-engineering of parts separately. For instance, a shorter top enclosure that enabled imaging at much closer distances to the sample (while maintaining the full petri dish imaging capabilities) can be developed (github.com/synbiouc/fluopi). For instance, this shorter top enclosure was used for the 6-day colony images shown in Fig 3E. This was developed mainly due to restrictions on the length of the CSI camera cable provided by the manufacturer (and incompatibilities with longer cables found in the market). An alternative to this would be mounting the adjustable focus M12 lens on a 3D-printed holder [59] designed for the Raspberry PI V2 camera sensor, which is compatible with longer cables. This would also allow increasing the image resolution from 5Mp to 8Mp. Our modular design approach will also help in accommodating further improvements such as multi-wavelength LED fast multicolor illumination switching [36], temperature control, or automated focus control [26].

Our project integrates software, hardware and wetware to achieve single-excitation multiple-emission fluorescence microscopy. The vast repertoire of available fluorescent proteins [60] permitted us to reduce the complexity of the hardware device, avoiding moving parts such as filter wheels. Moving filters increases not only the costs but also the risk of imaging artifacts due to vibration and movement of the sample during time lapse microscopy. The genetic components were designed following advanced standards for DNA assembly that allow for cheap, rapid and combinatorial assembly of genetic systems. These assembly standards are compatible with state-or-the-art genetic libraries such as CIDAR MoClo [45] and iGEM IIs [61], permitting users access to the latest DNA components.

In this project, we declare that we have no intentions to exert protection over the genetic resources used and aim to distribute them under an open material transfer agreement that is currently being drafted [62]. Free and open source wetware has just started to gain traction (e.g. OS pharma [63], OpenPlant, [64]); and together with open access to scientific publication, data, operational procedures, open hardware and FOSS, will make science and technology more accessible, reproducible, cost-effective and equitable [51, 65–67].

Building hardware, software and genetics from scratch leads to a better understanding of technologies and their integration. New educational modalities based on "tinkering" with biology, hardware and software for STEM training and capacity building have recently emerged (e.g. [68–72]. We provide examples of simple experimental setups that can be used in practical work involving the analysis of multiple gene expression, cell-cell signaling and microbial growth. We thus hope that this project will contribute to the democratization of science, technology and innovation in education.

Supporting information

S1 Fig. sfGFP expression by promoters of different strength: 1: J23100, 2: J23101, 3: J23107 and 4: J23116. BCD12 RBS and B0015 terminator was used for all the combinations.
(TIF)

S2 Fig. DNA electrophoresis gel imaging. Gel loaded with 20, 15, 10, 5, 4,3,2 and 1 l of 1 Kb Ladder (NEB) labelled with SYBR-Safe. and imaged using raspistill command: -t 5000 -ss 240000 -ISO 300 -awbg 1,1 -co 30. (B) using raspistill command: -t 5000 -ss 170000 -ISO 300 -awbg 1,1 -co 0.
(TIF)

S1 File. Assembly instructions for top and bottom enclosures.
(PDF)

S2 File. Assembly instructions for Raspberry Pi camera.
(PDF)

S3 File. Assembly instructions for camera system.
(PDF)

S4 File. Assembly instructions for PCB.
(PDF)

S5 File. Fluorescent signal mathematical analysis for time lapse images.
(PDF)

S6 File. Colony classification maths.
(PDF)

S1 Movie. Time lapse of diffusion assay for E. coli cells producing ("sender cells") and responding to ("receiver cells") C6 and C12 homoserine lactones plated on permeable membranes printed with hydrophobics grid lines.
(AVI)

S2 Movie. Time lapse of "star" diffusion assay for E. coli cells producing ("sender cells") and responding to ("receiver cells") C6 and C12 homoserine lactones plated on permeable membranes printed with hydrophobics grid lines (compressed for web streaming).
(AVI)

S3 Movie. Time lapse of sectoring colony growth (compressed for web streaming).
(AVI)

S4 Movie. Time lapse of mixed fluorescent bacteria (compressed for web streaming).
(AVI)

S5 Movie. Time lapse of growing E. coli labelled with sfGFP (compressed for web streaming).
(AVI)

S6 Movie. Time lapse of growing E. coli labelled with CyOFP.
(AVI)

S7 Movie. Time lapse of growing E. coli labelled with mBeRFP.
(AVI)

S8 Movie. Time lapse of mixed E. coli labelled with mBeRFP, sfGFP and mBeRFP.
(AVI)

Acknowledgments

Toby Wenzel for guidance on Docubricks documentation, Tom Baden for feedback and advice on camera, Bernardo Pollak for helping with sequences. Douglas Densmore for

the CIDAR MoClo Parts Kit. We would like to thank reviewers for very valuable comments.

Author Contributions

Conceptualization: Juan Keymer, Timothy Marzullo, Timothy Rudge, Fernán Federici.

Data curation: Isaac Nuñez, Tamara Matute.

Formal analysis: Isaac Nuñez, Tamara Matute, Timothy Rudge.

Funding acquisition: Juan Keymer, Timothy Marzullo, Timothy Rudge, Fernán Federici.

Investigation: Isaac Nuñez, Tamara Matute, Roberto Herrera, Timothy Rudge, Fernán Federici.

Methodology: Isaac Nuñez, Tamara Matute, Roberto Herrera.

Project administration: Timothy Marzullo, Timothy Rudge, Fernán Federici.

Resources: Tamara Matute, Roberto Herrera.

Software: Isaac Nuñez, Roberto Herrera.

Supervision: Timothy Marzullo, Timothy Rudge, Fernán Federici.

Validation: Juan Keymer.

Visualization: Fernán Federici.

Writing – original draft: Isaac Nuñez, Tamara Matute, Roberto Herrera, Timothy Rudge, Fernán Federici.

Writing – review & editing: Isaac Nuñez, Tamara Matute, Timothy Marzullo, Timothy Rudge, Fernán Federici.

References

1. Gibney E.'Open-hardware' pioneers push for low-cost lab kit. Nature. 2016; 531(7593):147–8. https://doi.org/10.1038/531147a PMID: 26961632
2. Baden T, Chagas AM, Gage G, Marzullo T, Prieto-Godino LL, Euler T. Open Labware: 3-D Printing Your Own Lab Equipment. PLOS Biol. 2015; 13(3):e1002086. https://doi.org/10.1371/journal.pbio.1002086 PMID: 25794301
3. Pearce JM. Building Research Equipment with Free, Open-Source Hardware. Science. 2012; 337 (6100):1303–1304. https://doi.org/10.1126/science.1228183 PMID: 22984059
4. Pearce J. M. Laboratory equipment: Cut costs with open-source hardware. Nature. 2014; 505 (7485), 618.
5. http://openpcr.org
6. Wittbrodt BT, Squires DA, Walbeck J, Campbell E, Campbell WH, Pearce JM. Open-Source Photometric System for Enzymatic Nitrate Quantification. PLoS ONE. 2015; 10(8): e0134989. https://doi.org/10.1371/journal.pone.0134989 PMID: 26244342
7. http://openqcm.com/scientific-papers
8. Marzullo TC, Gage GJ. The SpikerBox: a low cost, open-source bioamplifier for increasing public participation in neuroscience inquiry. PLoS One. 2012; 7(3):e30837. https://doi.org/10.1371/journal.pone.0030837 PMID: 22470415
9. OpenBCI [internet] http://openbci.com
10. Black C., Voigts J., Agrawal U., Ladow M., Santoyo J., Moore C., et al. Open Ephys electroencephalography (Open Ephys +EEG): a modular, low-cost, open-source solution to human neural recording. Journal of Neural Engineering. J Neural Eng. 2017 Jun; 14(3):035002. https://doi.org/10.1088/1741-2552/aa651f PMID: 28266930
11. PLoS ONE Open Labware collection [internet]. https://channels.plos.org/open-source-toolkit

12. Docubricks [internet]. http://docubricks.com
13. GitHUB [internet]. https://github.com
14. Thingiverse [internet]. https://www.thingiverse.com
15. Computadora Industrial Abierta Argentina [internet]. http://www.proyecto-ciaa.com.ar
16. Sharkey JP, Foo DCW, Kabla A, Baumberg JJ, Bowman RW. A one-piece 3D printed flexure translation stage for open-source microscopy. Rev Sci Instrum. 2016; 87(2): 25104.
17. Wijnen B, Hunt EJ, Anzalone GC, Pearce JM. Open-Source Syringe Pump Library. Gilestro GF, ed. *PLoS ONE*. 2014; 9(9):e107216. https://doi.org/10.1371/journal.pone.0107216 PMID: 25229451
18. Lam AT, Samuel-Gama KG, Griffin J, Loeun M, Gerber L, Hossain Z, et al. Device and programming abstractions for spatiotemporal control of active micro-particle swarms. Lab Chip. 2017; 17(8), 1442–1451. https://doi.org/10.1039/c7lc00131b PMID: 28322404
19. Miller AR, Davis GL, Oden ZM, Razavi MR, Fateh A, Ghazanfari M, et al. Portable, Battery-Operated, Low-Cost, Bright Field and Fluorescence Microscope. PLoS ONE. 2010; 5(8): e11890. https://doi.org/10.1371/journal.pone.0011890 PMID: 20694194
20. Nguyen V, Rizzo J, Sanii B. An Assemblable, Multi-Angle Fluorescence and Ellipsometric Microscope. PLoS ONE. 2016; 11(12): e0166735. https://doi.org/10.1371/journal.pone.0166735 PMID: 27907008
21. Pitrone PG, Schindelin J, Stuyvenberg L, Preibisch S, Weber M, Eliceiri KW, et al. OpenSPIM: an open-access light-sheet microscopy platform. Nat Meth. 2013; 10: 598–599. Public Policy. https://doi.org/10.1093/scipol/scv034
22. Gualda E. J., Vale T., Almada P., Feijó J. A., Martins G. G., Moreno N. OpenSpinMicroscopy: an open-source integrated microscopy platform. Nat. Methods 2013; 10, 599–600 https://doi.org/10.1038/nmeth.2508 PMID: 23749300
23. Rosenegger DG, Tran CHT, LeDue J, Zhou N, Gordon GR. A High Performance, Cost-Effective, Open-Source Microscope for Scanning Two-Photon Microscopy that Is Modular and Readily Adaptable. PLoS ONE. 2014; 9(10): e110475. https://doi.org/10.1371/journal.pone.0110475 PMID: 25333934
24. Campbell RAA, Eifert RW, Turner GC. Openstage: A Low-Cost Motorized Microscope Stage with Sub-Micron Positioning Accuracy. PLoS ONE. 2014; 9(2): e88977. https://doi.org/10.1371/journal.pone.0088977 PMID: 24586468
25. OpenLabTools GitHUB [internet]. http://openlabtools.eng.cam.ac.uk/Instruments/Microscope/
26. Chagas A. M., Godino L. P., Arrenberg A. B., & Baden T. The 100 Euro Lab: A 3-D Printable Open Source Platform For Fluorescence Microscopy, Optogenetics And Accurate Temperature Control During Behaviour Of Zebrafish, Drosophila And C. elegans. PLoS Biol. 2017 Jul 18; 15(7):e2002702. https://doi.org/10.1371/journal.pbio.2002702 PMID: 28719603
27. Switz NA, D'Ambrosio MV, Fletcher DA. Low-cost mobile phone microscopy with a reversed mobile phone camera lens. PLoS One. 2014 May 22; 9(5):e95330. https://doi.org/10.1371/journal.pone.0095330 PMID: 24854188
28. Phillips ZF, D'Ambrosio MV, Tian L, Rulison JJ, Patel HS, Sadras N, et al. Multi-Contrast Imaging and Digital Refocusing on a Mobile Microscope with a Domed LED Array. PLoS ONE. 2015; 10(5): e0124938. https://doi.org/10.1371/journal.pone.0124938 PMID: 25969980
29. Pirnstill CW, Coté GL. Malaria Diagnosis Using a Mobile Phone Polarized Microscope. Sci Rep. 2015 Aug 25; 5:13368. https://doi.org/10.1038/srep13368 PMID: 26303238
30. Wei Q, Acuna G, Kim S, Vietz C, Tseng D, Chae J, et al. Plasmonics Enhanced Smartphone Fluorescence Microscopy. Scientific Reports. 2017; 7:2124. https://doi.org/10.1038/s41598-017-02395-8 PMID: 28522808
31. PhoneScope [internet]. https://www.thingiverse.com/thing:280004
32. Liberti WA, Perkins LN, Leman DP, Gardner TJ. An open source, wireless capable miniature microscope system. Journal of Neural Engineering. 2017; 14(4), 45001. https://doi.org/10.1088/1741-2552/aa6806
33. Cybulski JS, Clements J, Prakash M. Foldscope: Origami-Based Paper Microscope. Martens L, ed. *PLoS ONE*. 2014; 9(6):e98781. https://doi.org/10.1371/journal.pone.0098781 PMID: 24940755
34. Magaraci MS, Bermudez JG, Yogish D, Pak DH, Mollov V, Tycko J, et al. Toolbox for Exploring Modular Gene Regulation in Synthetic Biology Training. ACS Synthetic Biology. 2016; 5(7), 781–785. http://doi.org/10.1021/acssynbio.6b00057 PMID: 27111289
35. OpenSpim Wiki [internet]. http://openspim.org/Welcome_to_the_OpenSPIM_Wiki
36. Bosse JB, Tanneti NS, Hogue IB, Enquist LW. Open LED Illuminator: A Simple and Inexpensive LED Illuminator for Fast Multicolor Particle Tracking in Neurons.PLoS One. 2015 Nov 23; 10(11):e0143547. https://doi.org/10.1371/journal.pone.0143547 PMID: 26600461

37. IORodeo transilluminator [internet]. https://iorodeo.com
38. Chu J, Oh Y, Sens A, Ataie N, Dana H, Macklin JJ, et al. A bright cyan-excitable orange fluorescent protein facilitates dual-emission microscopy and enhances bioluminescence imaging in vivo. Nat Biotechnol. 2016; 34: 760–767. https://doi.org/10.1038/nbt.3550 PMID: 27240196
39. Guan Y, Meurer M, Raghavan S, Rebane A, Lindquist JR, Santos S, et al. Live-cell multiphoton fluorescence correlation spectroscopy with an improved large Stokes shift fluorescent protein. Mol Biol Cell. 2015; 26: 2054–2066. https://doi.org/10.1091/mbc.E14-10-1473 PMID: 25877871
40. Yang J, Wang L, Yang F, Luo H, Xu L, Lu J, et al. mBeRFP, an improved large stokes shift red fluorescent protein. PLoS ONE. 2013; 8: e64849. https://doi.org/10.1371/journal.pone.0064849 PMID: 23840310
41. Lam AJ, St-Pierre F, Gong Y, Marshall JD, Cranfill PJ, Baird MA, et al. Improving FRET dynamic range with bright green and red fluorescent proteins. Nat Methods. 2012; 9: 1005–1012. https://doi.org/10.1038/nmeth.2171 PMID: 22961245
42. Ai HW, Henderson JN, Remington SJ, Campbell RE. Directed evolution of a monomeric, bright and photostable version of Clavularia cyan fluorescent protein: structural characterization and applications in fluorescence imaging. Biochem J. 2006 Dec 15; 400(3):531–40. https://doi.org/10.1042/BJ20060874 PMID: 16859491
43. Pédelacq JD, Cabantous S, Tran T, Terwilliger TC, Waldo GS. Engineering and characterization of a superfolder green fluorescent protein. Nature Biotechnology 2005; 24(1): 79–88 https://doi.org/10.1038/nbt1172 PMID: 16369541
44. Goedhart J, von Stetten D, Noirclerc-Savoye M, Lelimousin M, Joosen L, Hink MA. et al. Structure-guided evolution of cyan fluorescent proteins towards a quantum yield of 93%. Nature Communications. 2012; 3:751-. https://doi.org/10.1038/ncomms1738 PMID: 22434194
45. Iverson SV, Haddock TL, Beal J, Densmore DM. CIDAR MoClo: Improved MoClo Assembly Standard and New E. coli Part Library Enable Rapid Combinatorial Design for Synthetic and Traditional Biology. ACS Synth Biol. 2016 Jan 15; 5(1):99–103. https://doi.org/10.1021/acssynbio.5b00124 PMID: 26479688
46. Addgene MoClo kit [internet]. https://www.addgene.org/cloning/moclo/densmore/
47. Grant PK, Dalchau N, Brown JR, Federici F, Rudge TJ, Yordanov B, Patange O, Phillips A, Haseloff J. Orthogonal Intercellular Signaling for Programmed Spatial Behavior. Mol Syst Biol. 2016 Jan 25; 12 (1):849. https://doi.org/10.15252/msb.20156590 PMID: 26814193
48. Hallatschek O, Hersen P, Ramanathan S, Nelson DR. Genetic drift at expanding frontiers promotes gene segregation. Proc Natl Acad Sci U S A. 2007 Dec 11; 104(50):19926–30. https://doi.org/10.1073/pnas.0710150104 PMID: 18056799
49. Hol FJ, Galajda P, Woolthuis RG, Dekker C, Keymer JE. The idiosyncrasy of spatial structure in bacterial competition.BMC Res Notes. 2015 Jun 17; 8:245. https://doi.org/10.1186/s13104-015-1169-x PMID: 26081497
50. List of Open Hardware devices [internet] http://www.appropedia.org/Open-source_Lab
51. Zhang C, Anzalone NC, Faria RP, Pearce JM. Open-Source 3D-Printable Optics Equipment. PLoS One. 2013; 8(3):e59840. https://doi.org/10.1371/journal.pone.0059840 PMID: 23544104
52. Pearce JM. Return on Investment for Open Source Hardware Development. Science and Public Policy 2016; 43(2),192–195.
53. Gaudi Labs [internet] http://www.gaudi.ch/GaudiLabs/?page_id=2
54. Biohack Academy [internet] https://github.com/biohackacademy
55. Instructables [internet] http://www.instructables.com/contest/buildmylab/?show=ENTRIES
56. Hackteria [internet] http://wlu18www30.webland.ch/wiki/Collection_of_DIY_Biology,_Open_Source_Art_Projects
57. Hackaday [internet] http://hackaday.com
58. Hackteria DIY microscopy resources [internet] http://hackteria.org/wiki/DIY_microscopy
59. M12 lens holder file[internet] https://www.thingiverse.com/thing:1963856
60. UCSF site for fluorescent proteins [internet] http://nic.ucsf.edu/FPvisualization/
61. Golden Gate iGEM repository [internet] http://2016.igem.org/Resources/Plant_Synthetic_Biology/PhytoBricks
62. OpenMTA [internet] https://biobricks.org/openmta/
63. Open Source Pharma [internet] http://www.opensourcepharma.net
64. OpenPlant [internet] https://www.openplant.org

65. Pearce JM. Emerging Business Models for Open Source Hardware. Journal of Open Hardware 2017; 1 (1), p.2.

66. Nature Methods Editorial Board [internet] http://www.nature.com/nmeth/journal/v10/n7/full/nmeth.2554.html?foxtrotcallback=true

67. GOSH, Gathering For Open Science Hardware [internet] http://openhardware.science

68. Kim H, Gerber LC, Chiu D, Lee SA, Cira NJ, et al. Correction: LudusScope: Accessible Interactive Smartphone Microscopy for Life-Science Education. PLOS ONE 2016; 11(12): e0168053. https://doi.org/10.1371/journal.pone.0168053 PMID: 27936144

69. Teaching and Research in Natural Sciences for Development (TReND) in Africa [internet] www.TReNDinAfrica.org.

70. iGEM [internet] http://igem.org/Main_Page

71. Backyard Brains SpikerBox [internet] https://backyardbrains.com/products/emgspikerbox.

72. Karikari TK, Cobham AE, Ndams IS Building sustainable neuroscience capacity in Africa: the role of non-profit organisation. Metabolic brain disease 2016; 31:1, 3–9. https://doi.org/10.1007/s11011-015-9687-8 PMID: 26055077